

# **Unit Cell Volume, and Lattice Parameter of Cubic High Entropy Alloys**

J. Coreño Alonso<sup>a</sup>, O. Coreño Alonso<sup>a\*</sup>.

<sup>a</sup> Universidad de Guanajuato, Juárez # 77 Col. Centro, C.P. 36,000, Guanajuato, Gto. México.

\*ocoreno@ugto.mx.

## **Abstract.**

An equation has been derived to predict unit cell volume of high entropy alloys, HEA's, by two different methods. Both treatments led to the same equation. For cubic HEA's lattice parameters were calculated. The predicted lattice parameters were compared with those reported for 68 HEA's. Lattice parameters were also calculated using the equivalent of Vegard's law for these alloys. Average errors were 0.52%, and 0.42% when Vegard's law, and the equation derived in this work were used, respectively.

Preprint

## **1.- Introduction.**

High entropy alloys, HEA's, have received a lot of attention in recent years, and the possible use of high entropy alloys in diverse fields has been reported. Some of the possible applications are in catalysis [1], as ferromagnetic materials [2], in biomedical implants [3], in magnetocaloric refrigeration [4], as corrosion resistant materials [5], tribological materials [6], antiviral material [7], as an oxide dispersion-strengthened alloy [8], superconductor material [9], irradiation resistant materials [10], or as an alloy with transformation-induced plasticity [11].

Expressions to calculate lattice parameter in cubic binary or ternary intermetallics, with L1<sub>2</sub> [20] or B2 [17] structures, have been derived. From the equations in these references, an expression to calculate the unit cell volume of intermetallic compounds of any crystalline structure, and with any number of different solute element atoms was derived [21]. In this reference, it was proposed to take the element with highest concentration as the solvent. Data of intermetallic compounds with up to three elements were employed to evaluate the model. Good results were obtained with this approximation, even when solvent concentration was as low as 50% in some cases. If this approximation is to be applied to HEA's, a problem arises due to the difficulty to define the solvent when none of the elements has concentration higher

than 50%. In this work, two alternatives have been developed to tackle this problem. First, a HEA is considered as a mixture of solid solutions, later, a HEA is modeled as a mixture of solute element atoms surrounded by different environments. Both treatments led to the same equation to calculate unit cell volume. For cubic HEA's, lattice parameter can then be calculated. The predicted lattice parameters were compared with those reported for 68 HEA's.

## 2.- Equation to Calculate Unit Cell Volume for HEA'S Using Volume Size Factors.

Figure 1 shows a simplified scheme of a compact plane in a quaternary cubic HEA. It can be observed that atoms with the highest concentration, fifty percent, are blue. Red, black, and green atoms have half the ratio of blue atoms. In this figure, it is easy to identify the solvent element since it is the one with the highest concentration. Based on this figure, a HEA was considered as a mixture of solid solutions with different compositions. Then, an equation to calculate unit cell volume of the HEA was derived.

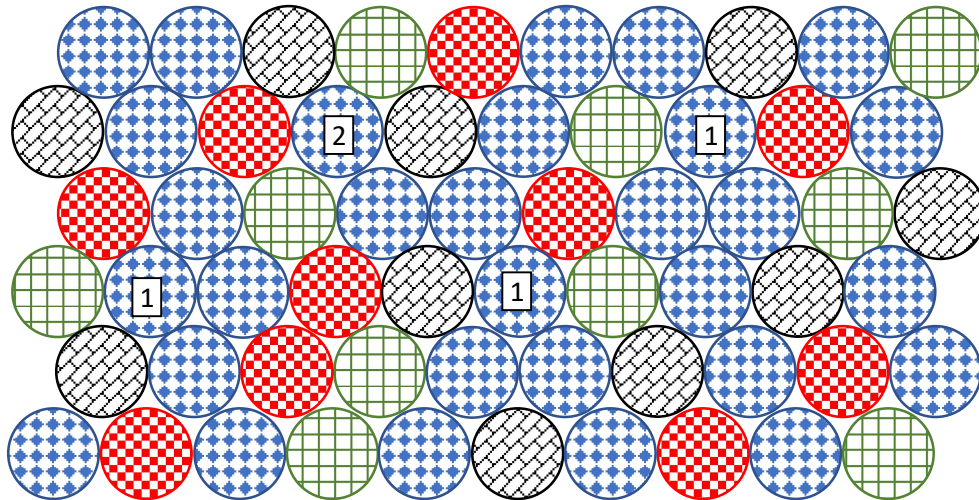


Figure 1. Simplified scheme of a compact plane in a quaternary cubic HEA.

The unit cell volume of a solid solution or intermetallic compound  $A_xB_yC_w.M_l$  can be expressed as [21]

$$V_{A_xB_yC_w...M_l} = Z \left( x\bar{V}_A + y\bar{V}_B + w\bar{V}_C + \dots + l\bar{V}_M \right) \quad (1)$$

$$\text{where } Z = \frac{\text{Number of atoms in the unit cell}}{(x+y+w+\dots+l)} \quad (2)$$

If the element A is considered as the solvent element, then, from the definition of volume size factor,  $\Omega_{sf}$ , [22] the effective atomic volume of element  $i$  in the solid solution,  $\bar{V}_i$ , can be expressed as

$$\bar{V}_i = V_A(1 + \Omega_{sf i/A}) \quad (3)$$

If (3) is replaced in (1) for each  $i$  element, then

$$V_{A_x B_y C_w M_l} = Z V_A [(x + y + w + \dots + l) + (y\Omega_{sf B/A} + w\Omega_{sf C/A} + \dots + l\Omega_{sf M/A})] = \\ \text{unit cell volume taking A as solvent element} \quad (4)$$

If B, C, or M are considered as the solvent element, then the volume of the unit cell of the solid solution can be expressed, respectively, as

$$V_{A_x B_y C_w \dots M_l} = Z V_B [(x + y + w + \dots + l) + (x\Omega_{sf A/B} + w\Omega_{sf C/B} + \dots + l\Omega_{sf M/B})] = \\ \text{unit cell volume taking B as solvent element} \quad (5)$$

$$V_{A_x B_y C_w \dots M_l} = Z V_C [(x + y + w + \dots + l) + (x\Omega_{sf A/C} + y\Omega_{sf B/C} + \dots + l\Omega_{sf M/C})] = \\ \text{unit cell volume taking C as solvent element} \quad (6)$$

•  
•

$$V_{A_x B_y C_w \dots M_l} = Z V_M [(x + y + w + \dots + l) + (x\Omega_{sf A/M} + y\Omega_{sf B/M} + w\Omega_{sf C/M} + \dots)] = \\ \text{unit cell volume taking M as solvent element} \quad (7)$$

Take  $c_i$  as the concentration of each element in the solid solution. If we consider the solid solution as a mixture of each solid solution (4) to (7), then the volume of the unit cell of this mixture is

$$V_{A_x B_y C_w \dots M_l} = c_A V \text{ unit cell A as solvent} + c_B V \text{ unit cell B as solvent} + \\ c_C V \text{ unit cell C as solvent} + \dots + c_M V \text{ unit cell M as solvent} \quad (8)$$

$$V_{A_x B_y C_w \dots M_l} = Z c_A V_A [(x + y + w + \dots + l) + (y\Omega_{sf B/A} + w\Omega_{sf C/A} + \dots + l\Omega_{sf M/A})]$$

$$+ Zc_B V_B [(x + y + w + \dots + l) + (x\Omega_{sfA/B} + w\Omega_{sfC/B} + \dots + l\Omega_{sfM/B})] + Zc_C V_C [(x + y + w + \dots + l) + (x\Omega_{sfA/C} + y\Omega_{sfB/C} + \dots + l\Omega_{sfM/C})] + \dots + Zc_M V_M [(x + y + w + \dots + l) + (x\Omega_{sfA/M} + y\Omega_{sfB/M} + w\Omega_{sfC/M+\dots})] \quad (9)$$

$$V_{A_xB_yC_w\dots M_l} = \text{Number of atoms in the unit cell} * [c_A V_A + c_B V_B + c_C V_C + \dots + c_M V_M] + \\ Zc_A V_A [y\Omega_{sfB/A} + w\Omega_{sfC/A} + \dots + l\Omega_{sfM/A}] + Zc_B V_B [x\Omega_{sfA/B} + w\Omega_{sfC/B} + \dots + l\Omega_{sfM/B}] + \\ Zc_C V_C [x\Omega_{sfA/C} + y\Omega_{sfB/C} + \dots + l\Omega_{sfM/C}] + \dots + Zc_M V_M [x\Omega_{sfA/M} + y\Omega_{sfB/M} + w\Omega_{sfC/M+\dots}] \quad (10)$$

For equiatomic high entropy alloys,  $c_i = c$  for all elements, and (10) can be simplified to

$$V_{A_xB_yC_w\dots M_l} = \text{Number of atoms in the unit cell} * c * [V_A + V_B + V_C + \dots + V_M] + Zc * \\ (V_A [y\Omega_{sfB/A} + w\Omega_{sfC/A} + \dots + l\Omega_{sfM/A}] + V_B [x\Omega_{sfA/B} + w\Omega_{sfC/B} + \dots + l\Omega_{sfM/B}] + \\ V_C [x\Omega_{sfA/C} + y\Omega_{sfB/C} + \dots + l\Omega_{sfM/C}] + \dots + V_M [x\Omega_{sfA/M} + y\Omega_{sfB/M} + w\Omega_{sfC/M+\dots}]) \quad (11)$$

Alternatively, the unit cell volume of the high entropy alloy could be derived considering each solute atom in the alloy.

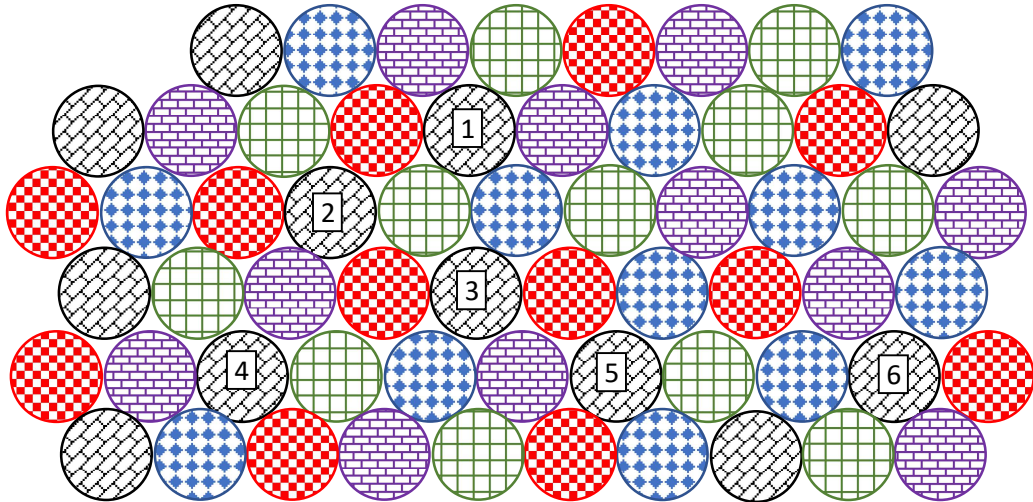


Figure 2. Simplified scheme of a compact plane in an equiatomic quinary cubic HEA.

In the solid solution  $A_xB_yC_w\dots M_l$ , the effective atomic volume,  $\bar{V}_l$ , of each solute element in the corresponding solvent is reported in Table 1.

Table 1. Effective atomic volume,  $\bar{V}_i$ , of each solvent element in the corresponding solute, in the solid solution  $A_xB_yC_{W..M_l}$ .

Solute \ Solvent	<i>A</i>	<i>B</i>	<i>C</i>	<i>M</i>
<i>A</i>	$V_A$	$V_B(1 + \Omega_{sfA/B})$	$V_C(1 + \Omega_{sfA/C})$	$V_M(1 + \Omega_{sfA/M})$
<i>B</i>	$V_A(1 + \Omega_{sfB/A})$	$V_B$	$V_C(1 + \Omega_{sfB/C})$	$V_M(1 + \Omega_{sfB/M})$
<i>C</i>	$V_A(1 + \Omega_{sfC/A})$	$V_B(1 + \Omega_{sfC/B})$	$V_C$	$V_M(1 + \Omega_{sfC/M})$
<i>M</i>	$V_A(1 + \Omega_{sfM/A})$	$V_B(1 + \Omega_{sfM/B})$	$V_C(1 + \Omega_{sfM/C})$	$V_M$

Given that the solvent elements concentrations are  $C_A$ ,  $C_B$ ,  $C_D$ , and  $C_M$ , the average atomic volume of each solute element,  $V_{i,av}$ , is

$$V_{A,av} = C_A V_A + C_B V_B(1 + \Omega_{sfA/B}) + C_C V_C(1 + \Omega_{sfA/C}) + \dots + C_M V_M(1 + \Omega_{sfA/M}) \quad (12)$$

$$V_{B,av} = C_A V_A(1 + \Omega_{sfB/A}) + C_B V_B + C_C V_C(1 + \Omega_{sfB/C}) + \dots + C_M V_M(1 + \Omega_{sfB/M}) \quad (13)$$

$$V_{C,av} = C_A V_A(1 + \Omega_{sfC/A}) + C_B V_B(1 + \Omega_{sfC/B}) + C_C V_C + \dots + C_M V_M(1 + \Omega_{sfC/M}) \quad (14)$$

$$V_{M,av} = C_A V_A(1 + \Omega_{sfM/A}) + C_B V_B(1 + \Omega_{sfM/B}) + C_C V_C(1 + \Omega_{sfM/C}) + \dots \quad (15)$$

Equations (12) - (15) would describe the average volume, that a solute atom has when it is surrounded by different number of atoms, of other elements. The high entropy solid solution would be described as a mixture of solute atoms, in several different surrounding environments.

The volume of each element in the unit cell, on average, is by  $C_i V_{i,av}$ , and the volume of the unit cell can be expressed as:

$$V_{A_xB_yC_{W..M_l}} = \text{Number of atoms in the unit cell} * [C_A V_{A,av} + C_B V_{B,av} + C_C V_{C,av} + \dots + C_M V_{M,av}] \quad (16)$$

Let us represent the *number of atoms in the unit cell* as *nauc*. Then,

$$\begin{aligned} V_{A_xB_yC_{W..M_l}} &= nauc * [C_A V_A + C_B V_B + C_C V_C + \dots + C_M V_M] * (C_A + C_B + C_C + \dots + C_M) + nauc * \\ &C_A V_A (C_B \Omega_{sfB/A} + C_C \Omega_{sfC/A} + \dots + C_M \Omega_{sfM/A}) + nauc * C_B V_B (C_A \Omega_{sfA/B} + C_B \Omega_{sfC/B} + \dots + \\ &C_M \Omega_{sfM/B}) + nauc * C_C V_C (C_A \Omega_{sfA/C} + C_B \Omega_{sfB/C} + \dots + C_M \Omega_{sfM/C}) + nauc * C_M V_M (C_A \Omega_{sfA/M} + \\ &C_B V_B \Omega_{sfB/M} + C_C \Omega_{sfC/M} + \dots) \end{aligned} \quad (17)$$

$$\text{Given that } C_A = x/(x + y + w + \dots + l), C_B = y/(x + y + w + \dots + l), C_C = w/(x + y + w + \dots + l), \dots, C_M = l/(x + y + w + \dots + l) \quad (18)$$

and that  $C_A + C_B + C_C + \dots + C_M = 1$  (19)

substituting (18) in (17), rearranging, and using (19), equation (10) is obtained again.

$$V_{A_xB_yC_W\dots M_l} = \text{Number of atoms in the unit cell} * [c_A V_A + c_B V_B + c_C V_C + \dots + c_M V_M] + \\ Zc_A V_A [y\Omega_{sfB/A} + w\Omega_{sfC/A} + \dots + l\Omega_{sfM/A}] + Zc_B V_B [x\Omega_{sfA/B} + w\Omega_{sfC/B} + \dots + l\Omega_{sfM/B}] + \\ Zc_C V_C [x\Omega_{sfA/C} + y\Omega_{sfB/C} + \dots + l\Omega_{sfM/C}] + \dots + Zc_M V_M [x\Omega_{sfA/M} + y\Omega_{sfB/M} + w\Omega_{sfC/M} \dots] \quad (10)$$

As can be seen, the same expression is obtained by the two methods described above.

### 3.- Discussion.

To evaluate equation (10), calculated values were compared with reported values of lattice parameters of 68 cubic HEA's. Unit cell volumes were converted to lattice parameters. Results are shown in Table 2. Volume size factors were taken from [22]. If they were not reported, they were calculated from crystallographic data. For eight systems crystallographic data were not found. Then,  $\Omega_{sf}$  was interpolated from the least square linear equation of  $\Omega_{sf}$  vs. solute atomic volume. This, for reported  $\Omega_{sf}$  values of the solvent element. The corresponding values are reported in Table 3.

Table 2. Reported, and calculated lattice parameters of HEA's, and the corresponding errors.

High Entropy Alloy	$a_0$ reported	$a_0$ Vegard's law	$a_0$ equation (10)	Vegard's law error	equation (10) error	$a_0$ determi- ned by	Chemical compo- sition by
W.273Nb.227Mo.256Ta.244 [23]	3.2134	3.2263	3.2148	0.401	0.044	XRD	ICP -OES
W.25Nb.22Mo.26Ta.27 [24]	3.24	3.23	3.22	0.309	0.617	XRD	EDS
NbMoTaW [25]	3.222	3.231	3.217	0.279	0.155	XRD	MNR
W.211Nb.206Mo.217Ta.156V.210 [23]	3.1832	3.1849	3.1804	0.053	0.088	XRD	ICP -OES
WNbMoTaVTi [26]	3.216	3.209	3.188	0.218	0.871	XRD Bragg's Law	EDS
CoFeReRu [27] v/z	25.482	25.585	25.436	0.404	0.180	XRD	MNR
CoCrFeNi [28]	3.575	3.579	3.587	0.112	0.336	XRD WPPM	MNR

						XRD WPPM	MNR
CoCrFeNiMn [28]	3.597	3.594	3.602	0.083	0.139	XRD WPPM	MNR
Co.204Cr.205Fe.202Mn.194Ni.195 [29]	3.59	3.59	3.6	0.000	0.279	XRD	EPMA
Co.203Cr.194Fe.206Mn.201Ni.196 [30]	3.60	3.59	3.60	0.278	0.000	XRD	XRF
Cr.127Fe.498Ni.111Mn.264 [31]	3.61	3.62	3.62	0.277	0.277	XRD	EDS
Co.20Cr.20Fe.40Ni.10Mn.10 [32]	3.587	3.598	3.605	0.307	0.502	XRD	MNR
Co.211Cr.187Fe.342Ni.063Mn.197 [33]	3.588	3.605	3.611	0.474	0.641	XRD	MNR
Ru.185Rh.156Pd.182Os.143Ir.159Pt.174 [34]	3.8473	3.8462	3.8471	0.029	0.005	XRD Rietveld	XRF
Ru.19Rh.20Re.21Os.21Ir.19 V/Z [35]	13.979	14.042	14.006	0.451	0.193	XRD Rietveld	EDS
NbZrHfVTi [36]	3.377	3.361	3.374	0.474	0.089	XRD Rietveld	MNR
Al.262Cr.241Fe.259Mo.235V.003 [37]	3.01	3.04	3.02	0.997	0.332	XRD *	EDS
Al.200Cr.243Fe.232Mo.166V.158 [37]	2.98	3.02	3.01	1.342	1.007	XRD*	EDS
Al.180Ni.189Cu.214Fe.196Cr.220 [38]	2.894	2.926	2.918	1.106	0.829	XRD	EDS
CoCrCuNiZn [39]	2.8831	2.9012	2.8815	0.628	0.056	XRD	MNR
NbZrHfTi [40]	3.438	3.435	3.428	0.087	0.291	XRD	MNR
Nb.200Mo.208Cr.187Ti.202V.203 [41]	3.140	3.139	3.138	0.032	0.064	XRD	EDS
NbTaTiV [42]	3.23	3.23	3.23	0.000	0.000	XRD	MNR
NbTaTiV [43]	3.2206	3.2319	3.2299	0.351	0.289	Neutron diffractio n, refined	MNR
Nb.27Mo.21Ta.27W.24 [44]	3.218	3.226	3.213	0.249	0.155	XRD Nelson- Riley regressio n	EDS
Nb.22Mo.18Ta.28W.31 [44]	3.216	3.222	3.210	0.187	0.187	XRD Nelson- Riley regressio n	EDS
Nb.24Mo.27Ta.25W.24 [44]	3.214	3.229	3.215	0.467	0.031	XRD Nelson- Riley regressio n	EDS
Nb.24Mo.18Ta.36W.22 [44]	3.228	3.245	3.234	0.527	0.186	XRD Nelson- Riley regressio n	EDS
Nb.216Mo.230Ta.281W.273 [45]	3.2034	3.2303	3.2177	0.840	0.446	XRD	EDS
Ti2ZrHfV0.5Mo0.2 [46]	3.4584	3.3805	3.3845	2.252	2.137	XRD	MNR
Ti.262Nb.255Ta.121Zr.242Al.120 [47]	3.355	3.363	3.360	0.238	0.149	XRD	EDS

V.098Co.301Cr.095Fe.455Ni.051 [48]	3.582	3.610	3.604	0.782	0.614	XRD	WCA
V.333Cr.309Fe.308Ta.025W.025 [49]	2.935	2.948	2.930	0.443	0.170	XRD Bragg's Law	EDS
Co.286Al.071Fe.286Ni.286Mn.071 [50]	3.6084	3.6061	3.5923	0.064	0.446	XRD	EDS
CoCrFeNiPd [51]	3.6473	3.6455	3.6658	0.049	0.507	XRD	MNR
CoCrFeNiPd [52]	3.6803	3.6455	3.6658	0.946	0.394	XRD full spectrum fitting	MNR
Co.244Cr.244Fe.244Ni.244Al.024 [53]	3.58	3.59	3.59	0.279	0.279	XRD	EDS
Co.314Al.029Fe.3181i.307Mn.032 [54]	3.5862	3.5798	3.5796	0.178	0.184	XRD	EDS
Co.290Al.067Fe.288Ni.268Mn.087 [54]	3.600	3.606	3.593	0.164	0.197	XRD	EDS
Co.2Al.1Fe.3Ni.4 [55]	3.5936	3.6132	3.5936	0.545	0.000	XRD	MNR
NbMoTaVTi [56]	3.1945	3.2153	3.2055	0.651	0.344	XRD Rietveld	MNR
Nb.199Hf.198Ta.175V.212Ti.217 [57]	3.279	3.295	3.290	0.488	0.336	XRD	EDS
Nb.304Mo.037Ta.0511Zr.29Ti.319 [58]	3.285	3.381	3.368	2.922	2.527	XRD at higher angle peaks	EDS
Nb.255Mo.207Ta.19Zr.131Ti.217 [58]	3.24	3.31	3.28	2.160	1.235	XRD at higher angle peaks	EDS
Nb.090Mo.0247Ta.032Zr.566Ti.289 [58]		3.36	3.34	1.818	1.212	TEM	EDS
Nb.275Mo.0947Ta.0911Zr.256Ti.284 [58]	3.40	3.47	3.46	2.059	1.765	TEM	EDS
NbZrHfVTi [59]	3.3663	3.3613	3.3582	0.148	0.241	Rietveld fullprof	MNR
Ir.191Pt.195Pd.207Rh.199Ru.208 [60]	3.856	3.849	3.851	0.182	0.130	XRD Rietveld	XRF
Co.237Cr.232Fe.245Ni.209Mn.077 [61]	3.58	3.59	3.59	0.279	0.279	XRD	EDS
Nb.238V.245Al.266Ti.251 [62]	3.18	3.07	3.1	3.459	2.516	XRD	MNR
Co.269Cr.250Fe.249Ni.184Mo.048 [63]	3.585	3.603	3.606	0.502	0.586	XRD (111) peak	EDS
Co.247Cr.245Fe.239Ni.246Mo.024 [64]	3.604	3.589	3.594	0.416	0.278	XRD Rietveld	EDS
Co.238Cr.2380Fe.238Ni.238Mo.048 [65]	3.595	3.599	3.602	0.111	0.195	Neutron diffraction	MNR
Co.204Cr.197Fe.299Ni.299 [66, 67]	3.5759	3.5764	3.5782	0.014	0.064	XRD (311) peak	EDS
Co.305Cr.208Fe.193Ni.294 [66, 67]	3.5695	3.5704	3.5721	0.025	0.073	XRD (311) peak	EDS
Co.296Cr.213Fe.303Ni.188 [66, 67]	3.5741	3.5801	3.5822	0.168	0.227	XRD (311) peak	EDS
Co.265Cr.205Fe.271Ni.260 [66, 67]	3.573	3.576	3.578	0.084	0.140	XRD (311)	EDS

						peak	
Co.220Cr.244Fe.230Ni.307 [66, 67]	3.5737	3.5758	3.577	0.059	0.092	XRD (311) peak	EDS
Co.229Cr.236Fe.325Ni.210 [66, 67]	3.5795	3.5834	3.5843	0.109	0.134	XRD (311) peak	EDS
Co.315Cr.245Fe.245Ni.220 [66, 67]	3.5704	3.6079	3.609	1.050	1.081	XRD (311) peak	EDS
Co.216Cr.227Fe.276Ni.281 [66, 67]	3.5752	3.5779	3.5792	0.076	0.112	XRD (311) peak	EDS
Co.277Cr.233Fe.233Ni.277 [66, 67]	3.572	3.5998	3.6013	0.778	0.820	XRD (311) peak	EDS
Co.273Cr.229Fe.284Ni.214 [66, 67]	3.5751	3.5801	3.5815	0.140	0.179	XRD (311) peak	EDS
Co.188Cr.214Fe.198Ni.400 [66, 67]	3.5708	3.5692	3.5711	0.045	0.008	XRD (311) peak	EDS
Co.201Cr.193Fe.400Ni.205 [66, 67]	3.5803	3.5847	3.5864	0.123	0.170	XRD (311) peak	EDS
Co.248Cr.244Fe.251Ni.257 [66, 67]	3.5767	3.5783	3.5793	0.045	0.073	XRD (311) peak	EDS
Co.386Cr.196Fe.211Ni.208 [66, 67]	3.568	3.5723	3.5744	0.120	0.179	XRD (311) peak	EDS

WCA = Wet chemical analysis.

MNR = Method used in analysis is not reported.

XRD\* = X ray diffraction, plot of  $h^2+k^2+l^2$  vs  $4Se\sin^2\theta/\lambda^2$ .

WPPM = Whole powder pattern modelling.

EDS = Energy dispersive spectroscopy.

XRD = X ray diffraction.

TEM = Transmission electron microscopy.

XRF = X ray fluorescence.

ICP-OES = Inductively coupled plasma -optical emission spectrometry.

EPMA = Electron probe microanalysis

Table 3. Volume size factors,  $\Omega_{sf}$  %, for systems not previously reported.

Solvent	Solute	$\Omega_{sf}$		Solvent	Solute	$\Omega_{sf}$
Al	Fe [68]	-47.65		Os	Ir [88]	1.74
	Mo [69]	-34.05			Pd [*]	4.77
	Nb [70]	4.48			Pt [89]	7.80
	Ni [71]	-22.60			Rh [90]	-1.63
Co	V [72]	4.54		Pt	Os [92]	-7.12
	Zn [73]	43.57				
				Re	Co [92]	-26.46
Cr	Cu [74]	3.33			Fe [93]	-23.94
	Ti [75]	46.17			Ir [94]	-5.61
	Zn [*]	26.50			Rh [95]	-6.70
Fe	Ta [76]	38.06		Rh	Os [96]	1.58

					Re [97]	4.17
Hf	Nb [77]	-19.95		Ru	Ru [98]	0.23
	Ta [78]	-19.63				
	Ti [*]	-21.24			Co [99]	-18.28
	V [*]	-40.81			Fe [100]	-11.24
	Zr [*]	4.31				
			Ta		Al [101]	-8.73
Ir	Re [79]	0.19			Fe [102]	-38.9
	Os [80]	-0.11			Hf [103]	21.93
Mo	Al [81]	-9.16	Ti		Nb [104]	1.49
	Co [83]	-30.11			W [105]	-17.11
	Fe [83]	-26.17				
	Ni [84]	-31.67	V		Hf [106]	64.64
	Zr [85]	23.11			Ni [107]	-27.83
				Ti [*]		26.22
Nb	Al [86]	-9.42				
	Cr [87]	-28.97	Zn		Cr [*]	-36.15
				Zr	Ta [*]	-25.02

\* Interpolated from the least square linear equation of  $\Omega_{sf}$  vs. solute atomic volume, for reported  $\Omega_{sf}$  values.

The first term in (10) is the equivalent of Vegard's law applied to HEA's. It is the unit cell volume produced by the average atomic volumes of the different elements in the alloy. The second term in (10) would represent the volume changes produced during alloy formation. On average, for the alloys analyzed in this work, it represents 1.27% of the reported experimental unit cell volumes. For ten alloys, it was between 2.51%, and 7.77%, and for 23 alloys it was higher than 1% of the average unit cell volume. So, volume changes produced during formation of HEA's must be considered when accurate values of cell volume or lattice parameters are required.

#### 4.- Conclusions.

An equation has been derived to predict unit cell volume of high entropy alloys by two different methods. In the first method, a HEA is considered as a mixture of solid solutions. Based on an equation previously reported to calculate unit cell volume of intermetallic compounds, an expression to calculate unit cell volume of HEA's was obtained. In the second method, a HEA is modeled as a mixture of solute element atoms surrounded by different environments. Using the effective volume of solute atoms in these environments, the unit cell

volume of a HEA was derived. Both treatments led to the same equation. For cubic HEA's lattice parameters were calculated. The predicted lattice parameters were compared with those reported for 68 HEA's. Lattice parameters were also calculated using the equivalent of Vegard's law for these alloys. Average errors were 0.52%, and 0.42% when Vegard's law, and the equation derived in this work were used, respectively. Although these average errors seem acceptable, they were as high as 3.46%, and 2.52% when Vegard's law, and the equation proposed are applied, respectively. The roles on error, of method to determine chemical composition, method to measure lattice parameter, and type of elements present on the alloy were examined.

## 5.- References.

1. K. Li, W. Chen, Recent progress in high-entropy alloys for catalysts: synthesis, applications, and prospects, *Materials Today Energy* 20 (2021) 100638.
2. Junjie Wang, Shangshu Wu, Shu Fu, Sinan Liu, Zhiqiang Ren, Mengyang Yan, Shuangqin Chen, Si Lan, Horst Hahn, Tao Feng, Nanocrystalline CoCrFeNiMn high-entropy alloy with tunable ferromagnetic properties, *Journal of Materials Science & Technology* 77 (2021) 126–130.
3. Muhammad Akmal, Ahtesham Hussain, Muhammad Afzal, Young Ik Lee, Ho Jin Ryu, Systematic Study of  $(\text{MoTa})_x\text{NbTiZr}$  Medium- and High-Entropy Alloys for Biomedical Implants- In Vivo Biocompatibility Examination, *Journal of Materials Science & Technology* 78 (2021) 183–191.
4. Zhihua Dong, Shuo Huang, Valter Ström, Guocai Chai, Lajos Károly Varga, Olle Eriksson, Levente Vitos,  $\text{MnxCr}0.3\text{Fe}0.5\text{Co}0.2\text{Ni}0.5\text{Al}0.3$  high entropy alloys for magnetocaloric refrigeration near room temperature, *Journal of Materials Science & Technology* 79 (2021) 15–20.
5. Yu Fu, Jun Li, Hong Luo, Cuiwei Du, Xiaogang Li, Recent advances on environmental corrosion behavior and mechanism of high-entropy alloys, *Journal of Materials Science & Technology* 80 (2021) 217–233.
6. Jie Xu, Xuan Kong, Minghui Chen \*, Qunchang Wang, Fuhui Wang, High-entropy FeNiCoCr alloys with improved mechanical and tribological properties by tailoring composition and controlling oxidation, *Journal of Materials Science & Technology* 82 (2021) 207–213.
7. Zhong Li, Dongxu Qiao, Yan Xu, Enze Zhou, Chuntian Yang, Xinyi Yuan, Yiping Lu, Ji-Dong Gu, Sand Wolfgang, Dake Xu, Fuhui Wang, Cu-bearing high-entropy alloys with excellent antiviral properties, *Journal of Materials Science & Technology* 84 (2021) 59–64.
8. SeungHyeok Chung, Bin Lee, Soo Yeol Lee, Changwoo Do, Ho Jin Ryu, The effects of Y pre-alloying on the in-situ dispersoids of ODS CoCrFeMnNi high-entropy alloy, *Journal of Materials Science & Technology* 85 (2021) 62–75.
9. Bin Liu, Jifeng Wu, Yanwei Cui, Qinqing Zhu, Guorui Xiao, Siqi Wu, Guang-han Cao, Zhi Ren, Structural evolution and superconductivity tuned by valence electron

concentration in the Nb-Mo-Re-Ru-Rh high-entropy alloys, *Journal of Materials Science & Technology* 85 (2021) 11–17.

10. Q. Xu1, H. Q. Guan, Z. H. Zhong, S. S. Huang, J. J. Zhao, Irradiation resistance mechanism of the CoCrFeMnNi equiatomic high-entropy alloy, *Scientific Reports* 11 (2021) 608.

11. Tianhao Wang, Shivakant Shukla, Bharat Gwalani, Subhasis Sinha, Saket Thapliyal, Michael Frank, Rajiv S. Mishra, *Scientific Reports* 11 (2021) 1579.

12. Ming-Hung Tsai, Jien-Wei Yeh, High-Entropy Alloys: A Critical Review, *Mat. Res. Lett.*, 2 (2014) 107-123.

13. Yong Zhang, Ting Ting Zuo, Zhi Tang, M. C. Gao, K. A. Dahmen, P. K. Liaw, Zhao Ping Liu, Microstructures and properties of high-entropy alloys, *Prog. Mater. Sci.*, 61 (2014) 1-93

14. Ming-Hung Tsai, Physical Properties of High Entropy Alloys, *Entropy*, 15 (2013) 5338-5345.

15. D.B. Miracle, O.N. Senkov, A critical review of high entropy alloys and related concepts, *Acta Materialia*, 122 (2017) 448-511.

16. Zhijun Wang, Qingfeng Wu, Wenquan Zhou, Feng He, Chunyan Yu, Deye Lin, Jincheng Wang, C.T. Liu, Quantitative determination of the lattice constant in high entropy alloys, *Scripta Materialia* 162 (2019) 468–471.

17. Bahatia ML, Singh AK, Nandy TK., Volume size factor and lattice parameter in cubic intermetallics with the B2 structure, *Intermetallics* 6 (1998) 141.

18. P. Haasen, “Physical Metallurgy”, R.W. Cahn, editor, North Holland, Amsterdam, 1965, p. 821.

19. D. B. SirdeshmukhL. SirdeshmukhK. G. Subhadra, Lattice Constant – A Solid State Probe. In: Micro- and Macro-Properties of Solids. Materials science, vol 80. Springer, Berlin, Heidelberg, (2006).

20. Bahatia ML, Singh AK, Nandy TK., Volume size factor and lattice parameter in cubic intermetallics with the L12 structure, *Intermetallics* 4 (1996) 635.

21. O. Coreño-Alonso, Unit cell volume of intermetallic compounds calculated using volume size factors, *Intermetallics* 14 (2006) 475–482.

22. H. W. King, Quantitative Size-Factors for Metallic Solid Solutions, *J. Matter. Sci.*, 1 (1966) 79.

23. O.N. Senkov, G.B. Wilks, D.B. Miracle, C.P. Chuang, P.K. Liaw, Refractory high-entropy alloys, *Intermetallics* 18 (2010) 1758-1765.

24. Hanuel Kim, Seungjin Nam, Aeran Roh, Myungwoo Son, Moon-Ho Ham, Jae-Hun Kim, Hyunjoo Choi, Mechanical and electrical properties of NbMoTaW refractory high-entropy alloy thin films, *International Journal of Refractory Metals & Hard Materials* 80 (2019) 286–291.

25. Yu Zou, Soumyadipta Maiti, Walter Steure, Ralph Spolenak, Size-dependent plasticity in an Nb<sub>25</sub>Mo<sub>25</sub>Ta<sub>25</sub>W<sub>25</sub> refractoryhigh-entropy alloy, *Acta Materialia* 65 (2014) 85–97.

26. B. Zhang, M. C. Gao, Y. Zhang, S. Yang and S. M. Guo, Senary refractory high entropy alloy, *Materials Science and Technology* 31 (2015) 1207.

27. M.C. Gao, B. Zhang, S.M. Guo, J.W. Qiao, J.A. Hawk, High-Entropy Alloys in Hexagonal Close-Packed Structure, *Metallurgical and Materials Transactions A*, 47 (2016) 3322.

28. Zaddach AJ, Niu C, Koch CC, Irving DL, Mechanical properties and stacking fault energies of NiFeCrCoMn high-entropy alloy, *JOM* 65(2013)1780–1789.
29. B. Cantor, I.T.H. Chang, P. Knight, A.J.B. Vincent, Microstructural development in equiatomic multicomponent alloys, *Materials Science and Engineering A* 375–377 (2004) 213–218.
30. G. Laplace, P. Gadaud, O. Horst, F. Otto, G. Eggeler, E.P. George, Temperature dependencies of the elastic moduli and thermal expansion coefficient of an equiatomic single-phase CoCrFeMnNi high-entropy alloy, *Journal of Alloys and Compounds*, 623 (2015) 348–353.
31. Raymond Kwesi Nutor, Q.P. Cao, X.D. Wang , D.X. Zhang, J.Z. Jiang, Tunability of the mechanical properties of (Fe50Mn27Ni10Cr13)100-xMoxhigh-entropy alloys via secondary phase control, *Journal of Materials Science & Technology* 73 (2021) 210–217.
32. Zemeng Yang, Dingshun Yan, Wenjun Lu, Zhiming Li, A TWIP-TRIP quinary high-entropy alloy: Tuning phase stability and microstructure for enhanced mechanical properties, *Materials Science & Engineering A* 801 (2021) 140441.
33. Wei Zhang, Zhichao Ma, Hongwei Zhao, Luquan Ren, Breakthrough the strength-ductility trade-off in a high-entropy alloy at room temperature via cold rolling and annealing, *Materials Science & Engineering A* 800 (2021) 140264.
34. Dongshuang Wu, Kohei Kusada, Tomokazu Yamamoto, Takaaki Toriyama, Syo Matsumura, Shogo Kawaguchi, Yoshiki Kubota, and Hiroshi Kitagawa, Platinum-Group-Metal High-Entropy-Alloy Nanoparticles, *Journal of the American Chemical Society* 142 (2020) 13833-13838.
35. Kirill V. Yusenko, Sephira Riva, Patricia A. Carvalho, Maria V. Yusenko, Serena Arnaboldi, Aleksandr S. Sukhikh, Michael Hanfland, Sergey A. Gromilov, First hexagonal close packed high-entropy alloy with outstanding stability under extreme conditions and electrocatalytic activity for methanol oxidation, *Scripta Materialia* 138 (2017) 22–27.
36. Victor Pacheco, Greta Lindwall, Dennis Karlsson, Johan Cedervall, Stefan Fritze, Gustav Ek, Pedro Berastegui, Martin Sahlberg, and Ulf Jansson, Thermal Stability of the HfNbTiVZr High-Entropy Alloy, *Inorg. Chem.* 58 (2019) 811–820.
37. Bharat Gwalani, Vishal Soni, Owais Ahmed Waseem, Srinivas Aditya Mantri, Rajarshi Banerjee, Laser additive manufacturing of compositionally graded AlCrFeMoVx ( $x = 0$  to 1) high-entropy alloy system, *Optics and Laser Technology* 113 (2019) 330–337.
38. A.I. Yurkova, V.V. Cherniavsky, V. Bolbut, M. Krüger, I. Bogomol, Structure formation and mechanical properties of the high-entropy AlCuNiFeCr alloy prepared by mechanical alloying and spark plasma sintering, *Journal of Alloys and Compounds* 786 (2019) 139–148.
39. Yuchen Sun, Boren Ke, Yulin Li, Kai Yang, Mingqi Yang, Wei Ji and Zhengyi Fu, Phases, Microstructures and Mechanical Properties of CoCrNiCuZn High-Entropy Alloy Prepared by Mechanical Alloying and Spark Plasma Sintering, *Entropy* 21 (2019) 122.
40. Jenő Gubicza, Anita Heczel, Megumi Kawasaki, Jae-Kyung Han, Yakai Zhao, Yunfei Xue, János L. Lábár, Evolution of microstructure and hardness in Hf25Nb25Ti25Zr25 high-entropy alloy during high-pressure torsion, *Journal of Alloys and Compounds* 788 (2019) 318–328.

41. C. Xiang, E.-H. Hanb, Z.M. Zhang, H.M. Fu, J.Q. Wang, H.F. Zhang, G.D. Hu, Design of single-phase high-entropy alloys composed of low thermal neutron absorption cross-section elements for nuclear power plant application, *Intermetallics* 104 (2019) 143–153.
42. Wenmin Guo, Bin Liu, Yong Liu, Tianchen Li, Ao Fu, Qihong Fang, Yan Nie, Microstructures and mechanical properties of ductile NbTaTiV refractory high entropy alloy prepared by powder metallurgy, *Journal of Alloys and Compounds* 776 (2019) 428-436.
43. F.X. Zhang, Y. Tong, M. Kirkham, A. Huq, H. Bei, W. J. Weber, Y.Zhang, Structural disorder, phase stability and compressibility of refractory body-centered cubic solid-solution alloys, *Journal of Alloys and Compounds* 847 (2020) 155970.
44. Michael Moorehead, Kaila Bertsch, Michael Niegoda, Calvin Parkin, Mohamed Elbakshwan,Kumar Sridharan, Chuan Zhang, Dan Thoma, Adrien Couet, High-throughput synthesis of Mo-Nb-Ta-W high-entropy alloys via additive manufacturing, *Materials and Design* 187 (2020) 108358
45. Hang Zhang, Yizhen Zhao, Sheng Huang, Shuo Zhu, Fu Wang and Dichen Li, Manufacturing and Analysis of High-Performance Refractory High-Entropy Alloy via Selective Laser Melting (SLM), *Materials* 12 (2019) 720.
46. Yiping Lu, Hefei Huang, Xuzhou Gao, Cuilan Ren, Jie Gao, Huanzhi Zhang, Shijian Zheng, Qianqian Jin, Yonghao Zhao, Chenyang Lu, Tongmin Wang, Tingju Li, A promising new class of irradiation tolerant materials:Ti2ZrHfV0.5Mo0.2 high-entropy alloy, *Journal of Materials Science & Technology* 35 (2019) 369–373.
47. Yuankui Cao, Yong Liu, Yunping Li, Bin Liu, Ao Fu, Yan Nie, Precipitation behavior and mechanical properties of a hot-worked TiNbTa0.5ZrAl0.5 refractory high entropy alloy, *International Journal of Refractory Metals & Hard Materials* 86 (2020) 105132.
48. Y.H. Jo, D.G. Kim, M.C. Jo, K.eY. Doh, S.S. Sohn, D. Lee, H.S. Kim, B.J. Lee,S. Lee, Effects of deformation induced BCC martensitic transformation and twinning on impact toughness and dynamic tensile response in metastable VCrFeCoNi high entropy alloy, *Journal of Alloys and Compounds* 785 (2019) 1056-1067.
49. Weiran Zhang, Peter K. Liaw and Yong Zhang, A Novel Low-Activation VCrFeTaxWx ( $x = 0.1, 0.2, 0.3, 0.4$ , and 1) High-Entropy Alloys with Excellent Heat-Softening Resistance, *Entropy* 20 (2018) 951.
50. Tiwen Lu, Tianbing He, Panpan Zhao, Kang Sun, Angelo F. Andreoli, Hongyu Chen,Weiping Chen, Zhiqiang Fu, Sergio Scudino, Fine tuning in-sync the mechanical and magnetic properties of FeCoNiAl0.25Mn0.25 high-entropy alloy through cold rolling and annealing treatment, *Journal of Materials Processing Tech.* 289 (2021) 116945.
51. M. S. Lucas, L. Mauger, J. A. Muñoz, Yuming Xiao, A. O. Sheets, S. L. Semiatin, J. Horwath, and Z. Turgut, Magnetic and vibrational properties of high-entropy alloys, *Journal of Applied Physics*, 109 (2011) 07E307.
52. Y.Tong, G.Velisa, S.Zhao, W.Guo, T.Yang, K.Jin, C.Lu, H.Bei, J.Y.P.Ko, D.C.Pagan, Y.Zhang, L.Wang, F.X.Zhang, Evolution of local lattice distortion under irradiation in medium- and high-entropy alloys, *Materialia* 2 (2018) 73-81.
53. Tiwen Lu, Tianbing He, Panpan Zhao, Kang Sun, Angelo F. Andreoli, Hongyu Chen, Weiping Chen, Zhiqiang Fu, Sergio Scudino, Fine tuning in-sync the mechanical and magnetic properties of FeCoNiAl0.25Mn0.25 high-entropy alloy through cold rolling and annealing treatment, *Journal of Materials Processing Tech.* 289 (2021) 116945.

54. Zhong Li, Guohua Bai, Xianguo Liu, Sateesh Bandaru, Zhongyuan Wu, Xuefeng Zhang, Mi Yan, Hui Xu, Tuning phase constitution and magnetic properties by composition in FeCoNiAlMn high-entropy alloys, *Journal of Alloys and Compounds* 845 (2020) 156203.
55. Zuozhe Niu, Ye Xie, Eugen Axinte, Juan Xu, Yan Wang, Development and characterization of novel Ni-rich high-entropy alloys, *Journal of Alloys and Compounds* 846 (2020) 156342.
56. F.X. Zhang, Y. Tong, M. Kirkham, A. Huq, H. Bei, W.J. Weber, Y. Zhang, Structural disorder, phase stability and compressibility of refractory body-centered cubic solid-solution alloys, *Journal of Alloys and Compounds* 847 (2020) 155970.
57. Zibing An, Shengcheng Mao, Yinong Liu, Li Wang, Hao Zhou, Bin Gan, Ze Zhang, Xiaodong Han, A novel HfNbTaTiV high-entropy alloy of superior mechanical properties designed on the principle of maximum lattice distortion *Journal of Materials Science & Technology* 79 (2021) 109–117.
58. Muhammad Akmal, Ahtesham Hussain, Muhammad Afzal, Young Ik Lee, Ho Jin Ryu, Systematic Study of (MoTa)<sub>x</sub>NbTiZr Medium- and High-Entropy Alloys for Biomedical Implants- In Vivo Biocompatibility Examination, *Journal of Materials Science & Technology* 78 (2021) 183–191.
59. Martin Sahlberg, Dennis Karlsson, Claudia Zlotea, Ulf Jansson, Superior hydrogen storage in high entropy alloys, *Sci. Rep.* 6 (2016) 36770.
60. Dongshuang Wu, Kohei Kusada, Tomokazu Yamamoto, Takaaki Toriyama, Syo Matsumura, Ibrahima Gueye, Okkyun Seo, Jaemyung Kim, Satoshi Hiroi, Osami Sakata, Shogo Kawaguchi, Yoshiaki Kubota, Hiroshi Kitagawa, On the electronic structure and hydrogenevolution reaction activity of platinum groupmetal-based high-entropy-alloy nanoparticles, *Chem. Sci.* 11 (2020) 12731.
61. Koželj, S. Vrtnik, M. Krnel, A. Jelen, D. Gačnik, M. Wencka, Z. Jagličić, A. Meden, F. Danoix, J. Ledieu, M. Feuerbacher, J. Dolinšek, Spin-glass magnetism of the non-equiautomic CoCrFeMnNi high-entropy alloy, *Journal of Magnetism and Magnetic Materials* 523 (2021) 167579.
62. N.D. Stepanov, D.G. Shaysultanov, G.A. Salishchev, M.A. Tikhonovsky, Structure and mechanical properties of a light-weight AlNbTiV high entropy alloy, *Materials Letters*, 142 (2015) 153–155.
63. W.H. Liu, Z.P. Lu, J.Y. He, J.H. Luan, Z.J. Wang, B. Liu, Yong Liu, M.W. Chen, C. T. Liu, Ductile CoCrFeNiMox high entropy alloys strengthened by hard intermetallic phases. *Acta Materialia*, 116 (2016) 332-342.
64. Biao Cai, Bin Liu, Saurabh Kabra, Yiqiang Wang, Kun Yan, Peter D. Lee, Yong Liu, Deformation mechanisms of Mo alloyed FeCoCrNi high entropy alloy: In situ neutron diffraction, *Acta Materialia* 127 (2017) 471-480.
65. Lei Tang, Kun Yan, Biao Cai, Yiqiang Wang, Bin Liu, Saurabh Kabra, Moataz M. Attallah, Yong Liu, Deformation mechanisms of FeCoCrNiMo0.2 high entropy alloy at 77 and 15 K, *Scripta Materialia* 178 (2020) 166–170.
66. Zhijun Wang, Qingfeng Wu, Wenquan Zhou, Feng He, Chunyan Yu, Deye Lin, Jincheng Wang, C.T. Liu, Quantitative determination of the lattice constant in high entropy alloys, *Scripta Materialia* 162 (2019) 468–471.

67. Feng He, Zhijun Wang, Qingfeng Wu, Sizhe Niu, Junjie Li, Jincheng Wang, C.T. Liu, Solid solution island of the Co-Cr-Fe-Ni high entropy alloy system, Scripta Materialia 131 (2017) 42–46.
68. [https://materials.springer.com/lb/docs/sm\\_lbs\\_978-3-540-39444-0\\_104](https://materials.springer.com/lb/docs/sm_lbs_978-3-540-39444-0_104)
69. [https://materials.springer.com/isp/crystallographic/docs/sd\\_1301287](https://materials.springer.com/isp/crystallographic/docs/sd_1301287)
70. [https://materials.springer.com/lb/docs/sm\\_lbs\\_978-3-540-39444-0\\_123](https://materials.springer.com/lb/docs/sm_lbs_978-3-540-39444-0_123)
71. [https://materials.springer.com/isp/crystallographic/docs/sd\\_0532459](https://materials.springer.com/isp/crystallographic/docs/sd_0532459)
72. [https://materials.springer.com/isp/crystallographic/docs/sd\\_0533747](https://materials.springer.com/isp/crystallographic/docs/sd_0533747)
73. [https://materials.springer.com/isp/crystallographic/docs/sd\\_1013216](https://materials.springer.com/isp/crystallographic/docs/sd_1013216)
74. [https://materials.springer.com/isp/crystallographic/docs/sd\\_1803194](https://materials.springer.com/isp/crystallographic/docs/sd_1803194)
75. [https://materials.springer.com/isp/crystallographic/docs/sd\\_0450079](https://materials.springer.com/isp/crystallographic/docs/sd_0450079)
76. [https://materials.springer.com/isp/crystallographic/docs/sd\\_0531990](https://materials.springer.com/isp/crystallographic/docs/sd_0531990)
77. [https://materials.springer.com/isp/crystallographic/docs/sd\\_0250232](https://materials.springer.com/isp/crystallographic/docs/sd_0250232)
78. [https://materials.springer.com/isp/crystallographic/docs/sd\\_0531897](https://materials.springer.com/isp/crystallographic/docs/sd_0531897)
79. [https://materials.springer.com/isp/crystallographic/docs/sd\\_1815137](https://materials.springer.com/isp/crystallographic/docs/sd_1815137)
80. [https://materials.springer.com/isp/crystallographic/docs/sd\\_0250662](https://materials.springer.com/isp/crystallographic/docs/sd_0250662)
81. [https://materials.springer.com/isp/crystallographic/docs/sd\\_0451296](https://materials.springer.com/isp/crystallographic/docs/sd_0451296)
82. [https://materials.springer.com/isp/crystallographic/docs/sd\\_0451570](https://materials.springer.com/isp/crystallographic/docs/sd_0451570)
83. [https://materials.springer.com/isp/crystallographic/docs/sd\\_0451196](https://materials.springer.com/isp/crystallographic/docs/sd_0451196)
84. [https://materials.springer.com/isp/crystallographic/docs/sd\\_1251285](https://materials.springer.com/isp/crystallographic/docs/sd_1251285)
85. [https://materials.springer.com/isp/crystallographic/docs/sd\\_0261267](https://materials.springer.com/isp/crystallographic/docs/sd_0261267)
86. [https://materials.springer.com/isp/crystallographic/docs/sd\\_0311646](https://materials.springer.com/isp/crystallographic/docs/sd_0311646)
87. [https://materials.springer.com/isp/crystallographic/docs/sd\\_0534143](https://materials.springer.com/isp/crystallographic/docs/sd_0534143)
88. [https://materials.springer.com/isp/crystallographic/docs/sd\\_0250659](https://materials.springer.com/isp/crystallographic/docs/sd_0250659)
89. [https://materials.springer.com/isp/crystallographic/docs/sd\\_1023867](https://materials.springer.com/isp/crystallographic/docs/sd_1023867)
90. [https://materials.springer.com/isp/crystallographic/docs/sd\\_1622247](https://materials.springer.com/isp/crystallographic/docs/sd_1622247)
91. [https://materials.springer.com/isp/crystallographic/docs/sd\\_0250661](https://materials.springer.com/isp/crystallographic/docs/sd_0250661)
92. [https://materials.springer.com/isp/crystallographic/docs/sd\\_1421145](https://materials.springer.com/isp/crystallographic/docs/sd_1421145)
93. [https://materials.springer.com/isp/crystallographic/docs/sd\\_0260610](https://materials.springer.com/isp/crystallographic/docs/sd_0260610)
94. [https://materials.springer.com/isp/crystallographic/docs/sd\\_1639567](https://materials.springer.com/isp/crystallographic/docs/sd_1639567)
95. [https://materials.springer.com/isp/crystallographic/docs/sd\\_1933779](https://materials.springer.com/isp/crystallographic/docs/sd_1933779)
96. [https://materials.springer.com/isp/crystallographic/docs/sd\\_1907168](https://materials.springer.com/isp/crystallographic/docs/sd_1907168)
97. [https://materials.springer.com/isp/crystallographic/docs/sd\\_1819814](https://materials.springer.com/isp/crystallographic/docs/sd_1819814)
98. [https://materials.springer.com/lb/docs/sm\\_lbs\\_978-3-540-70705-9\\_2609](https://materials.springer.com/lb/docs/sm_lbs_978-3-540-70705-9_2609)
99. [https://materials.springer.com/isp/crystallographic/docs/sd\\_0261240](https://materials.springer.com/isp/crystallographic/docs/sd_0261240)
100. [https://materials.springer.com/isp/crystallographic/docs/sd\\_0547974](https://materials.springer.com/isp/crystallographic/docs/sd_0547974)
101. [https://materials.springer.com/isp/crystallographic/docs/sd\\_0261788](https://materials.springer.com/isp/crystallographic/docs/sd_0261788)
102. [https://materials.springer.com/isp/crystallographic/docs/sd\\_0456760](https://materials.springer.com/isp/crystallographic/docs/sd_0456760)
103. [https://materials.springer.com/isp/crystallographic/docs/sd\\_0531897](https://materials.springer.com/isp/crystallographic/docs/sd_0531897)
104. [https://materials.springer.com/isp/crystallographic/docs/sd\\_0532178](https://materials.springer.com/isp/crystallographic/docs/sd_0532178)
105. Trans. Metall. Soc. AIME, 242, 1968, 953-954
106. [https://materials.springer.com/isp/crystallographic/docs/sd\\_0453747](https://materials.springer.com/isp/crystallographic/docs/sd_0453747)
107. [https://materials.springer.com/isp/crystallographic/docs/sd\\_0451215](https://materials.springer.com/isp/crystallographic/docs/sd_0451215)
108. L. Vegard, DieKonstitution der Mischkristalle und die Raumfillüng der Atome, Z. fur Physik 5 (1921) 17.

109. Victor Pacheco, Greta Lindwall, Dennis Karlsson, Johan Cedervall, Stefan Fritze, Gustav Ek, Pedro Berastegui, Martin Sahlberg, and Ulf Jansson, Thermal Stability of the HfNbTiVZr High-Entropy Alloy, *Inorg. Chem.* 58 (2019) 811–820.
110. B. Zhang, M. C. Gao, Y. Zhang, S. Yang and S. M. Guo, Senary refractory high entropy alloy, *Materials Science and Technology* 31 (2015) 1207.
111. Yu Zou, Soumyadipta Maiti, Walter Steure, Ralph Spolenak, Size-dependent plasticity in an Nb<sub>25</sub>Mo<sub>25</sub>Ta<sub>25</sub>W<sub>25</sub> refractoryhigh-entropy alloy, *Acta Materialia* 65 (2014) 85–97.
112. Michael Moorehead, Kaila Bertsch, Michael Niezgoda, Calvin Parkin, Mohamed Elbakhshwan, Kumar Sridharan, Chuan Zhang, Dan Thoma, Adrien Couet, High-throughput synthesis of Mo-Nb-Ta-W high-entropy alloys via additive manufacturing, *Materials and Design* 187 (2020) 108358.
113. J. Goldstein, D. E. Newbury, C. Joy, Ch. E. Lyman, P. Echlin, E. Lifshin, L. Sawyer, J. R. Michael, *Scanning Electron Microscopy and X-Ray Microanalysis*: Third Edition, Kluwer Academic/Plenum Publishers, New York, 2003, p. 193.
114. W.B. Pearson, *A Handbook of Lattice Spacings and Structures of Metals and Alloys*— pg 6, Pergamon Press, 1958.
115. Gschneider Jr. KA. In: Bennet LH, editor. *Theory of alloy phase formation*. The Metals Society of AIME, 1980, p. 1. Zhijun Wang, Qingfeng Wu, Wenquan Zhou, Feng He, Chunyan Yu, Deye Lin, Jincheng Wang, C.T. Liu, Quantitative determination of the lattice constant in high entropy alloys, *Scripta Materialia* 162 (2019) 468–471.